JACS
JOURNAL OF THE AMERICAN CHEMICAL SOCIETY
Article
pubs.acs.org/JACS

(2 + 2) Cycloaddition of Benzyne to Endohedral Metallofullerenes $M_3N@C_{80}$ (M = Sc, Y): A Rotating-Intermediate Mechanism

Tao Yang,[†,‡] Shigeru Nagase,[§] Takeshi Akasaka,[∥] Josep M. Poblet,[⊥] K. N. Houk,*[,#] Masahiro Ehara,[‡] and Xiang Zhao*[,†]

[†]Institute for Chemical Physics & Department of Chemistry, Xi'an Jiaotong University, Xi'an 710049, China
[‡]Institute for Molecular Science, Okazaki 444-8585, Japan
[§]Fukui Institute for Fundamental Chemistry, Kyoto University, Kyoto 606-8103, Japan
[∥]Department of Chemistry, Tokyo Gakugei University, Tokyo 184-8501, Japan
[⊥]Department de Química Físicai Inorgànica, Universitat Rovira i Virgili, 43007 Tarragona, Spain
[#]Department of Chemistry and Biochemistry, University of California, Los Angeles, California 90095-1569, United States

Supporting Information

ABSTRACT: The reaction mechanism and origin of regioselectivity of (2 + 2) cycloadditions of benzyne to endohedral metallofullerenes $M_3N@C_{80}$ (M = Sc, Y) were investigated with density functional calculations. The reaction was demonstrated to follow a diradical mechanism rather than a carbene mechanism, in which the formation of the diradical intermediate is the rate-determining step. Through rotation of benzyne moiety on the fullerene surface, the diradical intermediate on 566 site could isomerize to two new diradical intermediates which give rise to two distinct [5,6] and [6,6] benzoadducts, respectively. However, the diradical intermediate on 666 site only produces the [6,6] benzoadduct. The nature of the endohedral cluster not only influences the regioselectivity, but also determines the cycloadduct geometry. For $Sc_3N@C_{80}$, the [5,6] benzoadduct is preferred kinetically and thermodynamically, whereas in the case of $Y_3N@C_{80}$, both [5,6] and [6,6] benzoadducts are favorable. In contrast to closed-cage benzoadducts of $Sc_3N@C_{80}$, $Y_3N@C_{80}$ affords open-cage benzoadducts, making it the first example that the endohedral cluster could alter cycloadducts from the closed cage to open cage. With further analysis, it is revealed that the origin of regioselectivity results from the local strain energy of the fullerene cage.

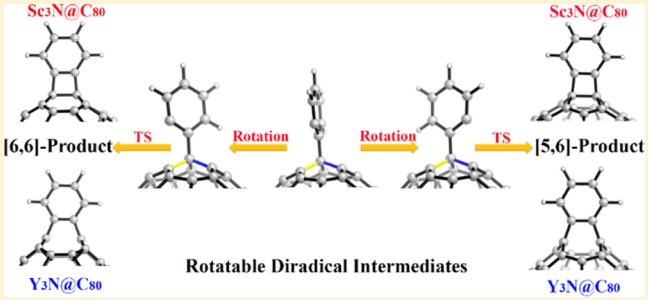

INTRODUCTION

Endohedral metallofullerenes (EMFs), which are the novel derivatives of fullerenes with metal atom(s) or clusters encapsulated inside, exhibit fascinating properties and have promising applications in fields, such as biomedicine and materials science.[1] Chemical modification of EMFs provides opportunities to tune their physical and chemical properties for potential applications and has received significant attention from the scientific community.[1,2] The availability of various chemical reactions, like Diels–Alder reaction, 1,3-dipolar cycloaddition, photochemical silylation, carbene additions, Bingel-Hirsch reaction, and (2 + 2) cycloaddition, has been exploited to attach organic molecules with various functionalities on the external surfaces of EMFs.[3]

(2 + 2) cycloadditions of aryne, which take place with pristine fullerenes C_{60} and C_{70},[4] have been realized upon EMFs such as $Sc_3N@C_{80}$, $La@C_{82}$, and $Gd@C_{82}$,[5] resulting in thermally stable isomeric cycloadducts with potential applications in molecular electronics and solar cell construction. For example, due to the fast rotation of endohedral cluster, $Sc_3N@I_h$-C_{80} exhibits only two nonequivalent carbon bonds, the [5,6] ring junction and the [6,6] ring junction. Interestingly, cycloaddition of aryne to $Sc_3N@C_{80}$ produces both [5,6] and [6,6] cycloadducts without any interconversion even in very high temperature,[5c,d] though the [5,6] cycloadduct is always more favorable than the [6,6] cycloadduct for $Sc_3N@C_{80}$.[3c,g,6] More importantly, thanks to the exohedral benzyne addition, the dynamics and electronic properties of the Sc_3N cluster are significantly tuned.[7]

Three possible reaction pathways, **a**, **b**, and **c**, have been proposed in the literature to account for (2 + 2) cycloaddition in organic chemistry, as shown in Scheme 1. The direct concerted pathway **a**, which is forbidden by the Woodward–Hoffmann rules,[8] can be excluded. Pathway **b** proceeds through the formation of a cyclopropylcarbene intermediate followed by ring expansion.[9,10] Pathway **c** involves a singlet diradical intermediate and a ring-closing step.[9,10] The reaction mechanism of (2 + 2) cycloaddition strongly depends on the reactants involved. Cycloaddition of ethylene to cyclopentyne

Received: February 9, 2015
Published: May 13, 2015

DOI: 10.1021/jacs.5b01444
J. Am. Chem. Soc. 2015, 137, 6820–6828

Scheme 1. Three Possible Reaction Mechanisms for the (2 + 2) Cycloaddition of Benzyne to EMFs

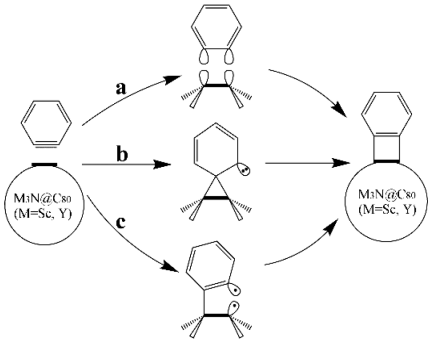

occurs by the carbene pathway rather than the diradical pathway,[9,10] whereas the diradical pathway is favored for (2 + 2) cycloaddition of ethylene and benzyne as well as 1,6-fullerenynes.[10,11] Moreover, the carbene pathway does not occur[12] in the intramolecular (2 + 2) cycloaddition of allene-ynes or the cyclotrimerization of fluoro- and chloroacetylenes. The mechanistic study of the (2 + 2) cycloadditions of aryne with fullerenes or EMFs is rare, and this prevents understanding of the functionalization of fullerenes or EMFs for special applications.

In addition to the reaction mechanism, the effect of the endohedral metallic cluster is also very important. Previous studies on Diels–Alder and 1,3-dipolar cycloadditions of $M_3N@C_{80}$[3c,g,6,13] showed that the exohedral chemical reactivity and regioselectivity are significantly affected by the nature of the metallic cluster. The [5,6] cycloadduct is preferred for $M_3N@C_{80}$ (M = Sc, Lu), whereas in the case of $M_3N@C_{80}$ (M = Y, Gd) with larger and more electropositive metal atoms, the [6,6] cycloadduct competes with the [5,6] cycloadduct. For the (2 + 2) cycloaddition on $M_3N@C_{80}$, the role of the metallic cluster on the reaction mechanism, selectivity, and cycloadduct geometry are all unclear.

We report density functional theory (DFT) calculations on (2 + 2) cycloaddition of benzyne with $M_3N@C_{80}$ (M = Sc, Y). Our work explores the reaction mechanism and the effect of the endohedral metallic cluster, and reveals the origin of the regioselectivity.

■ COMPUTATIONAL METHODS

The molecular geometries were optimized at the (U)B3LYP/Lanl2dz~6-31G(d) level of theory in the gas phase; the 6-31G(d) basis set was used for H, C, and N, while the Lanl2dz was used for Sc and Y.[14,15] All the structures were verified by the frequency calculations to be local minima or have one (and only one) imaginary frequency. The triplet diradical pathways are higher in energy.

Though B3LYP was revealed to underestimate the reaction energetics,[16] it has been demonstrated that for the diradical involved reactions B3LYP can even provide results similar to those from more computationally demanding *ab initio* methods such as coupled cluster method CCSD,[17] CACCSF,[18] and full CI.[9,10] Thus, B3LYP has been widely used to compute singlet/triplet energy gaps and to study the singlet diradicals involved molecules and chemical reactions, including (2 + 2) cyclo-additions.[9,10,19]

Very recently, Haberhauer and co-workers used double-hybrid method B2PLYPD[20] and CCSD(T) to investigate the diradical involved reactions and obtained very good energetics close to experimental results.[21] To further confirm the reliability of B3LYP for diradical involved (2 + 2) cycloaddition, we performed comprehensive calculations on a simply analogical system, (2 + 2) cycloaddition of benzyne with ethylene. It is found that B3LYP gives good geometries and close activation and reaction energetics to the B2PLYPD.[22]

In order to further evaluate the energetics of (2 + 2) cycloaddition of benzyne and EMFs, single-point energy calculations were performed by using B3LYP, B3LYPD,[20,23] B3LYP-D3 (Becke-Johnson damping, BJ),[24] and mPW1PW91[25] with Lanl2dz for metal atoms and 6-311G(d,p) for all other atoms. The B3LYP and B3LYP-D3 results are discussed in the present work, while B3LYPD and mPW1PW91 results are collected in the Supporting Information (SI). We also calculated several intermediates and transition states by employing Lanl2dz and 6-311+G(d,p) basis sets and the results showed that the relative energy differences are less than 0.5 kcal/mol. The electron charge states were obtained with the natural bond orbital (NBO)[26] analysis at the B3LYP/Lanl2dz~6-311G(d,p) level.

The ΔE is the relative electronic energies without any corrections, while ΔG represents relative Gibbs free energies involving zero-point vibrational energies (ZPVE) and thermal corrections at 298 K. All the density functional calculations were carried out with Gaussian 09 program.[27] The Grimme's DFT-D3 dispersion corrections were calculated using the DFTD3 program.[28] Figures 1, 2, 4, and 8 were drawn with CYLView.[29]

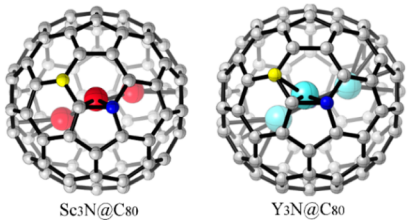

Figure 1. Two possible sites for the first addition step of benzyne to $M_3N@C_{80}$ (M = Sc, Y), 566 (blue) and 666 (yellow) sites.

■ RESULTS AND DISCUSSION

First, we focused on the carbene intermediate and three-numbered ring, which is the key structure of pathway **b**. No local minima could be located for such a carbene intermediate. Furthermore, by scanning the bond distance between benzyne and EMF, we found that when benzyne approaches the EMF and forms a three-numbered ring, the relative energy increases and is always higher than the isolated benzyne and EMF (please see SI for more details). Consequently, the carbene intermediates does not exist, and the cycloaddition reaction could proceed through the diradical mechanism, pathway **c**. Figure 1 illustrates two possible addition sites for the first step of benzyne addition, 566 and 666, one of which is surrounded by one pentagon and two hexagons while the other is in the center of three hexagons.

1. Reaction Mechanism of the (2 + 2) Cycloaddition of Benzyne to $Sc_3N@C_{80}$. As displayed in Figure 2, the benzyne addition to $Sc_3N@C_{80}$ begins by formation of a single carbon bond between benzyne with 566 or 666 site, $\mathbf{TS}_{1,566}$ and $\mathbf{TS}_{1,666}$. Compared with $\mathbf{TS}_{1,666}$, the energy barrier of $\mathbf{TS}_{1,566}$ is

DOI: 10.1021/jacs.5b01444
J. Am. Chem. Soc. 2015, 137, 6820–6828

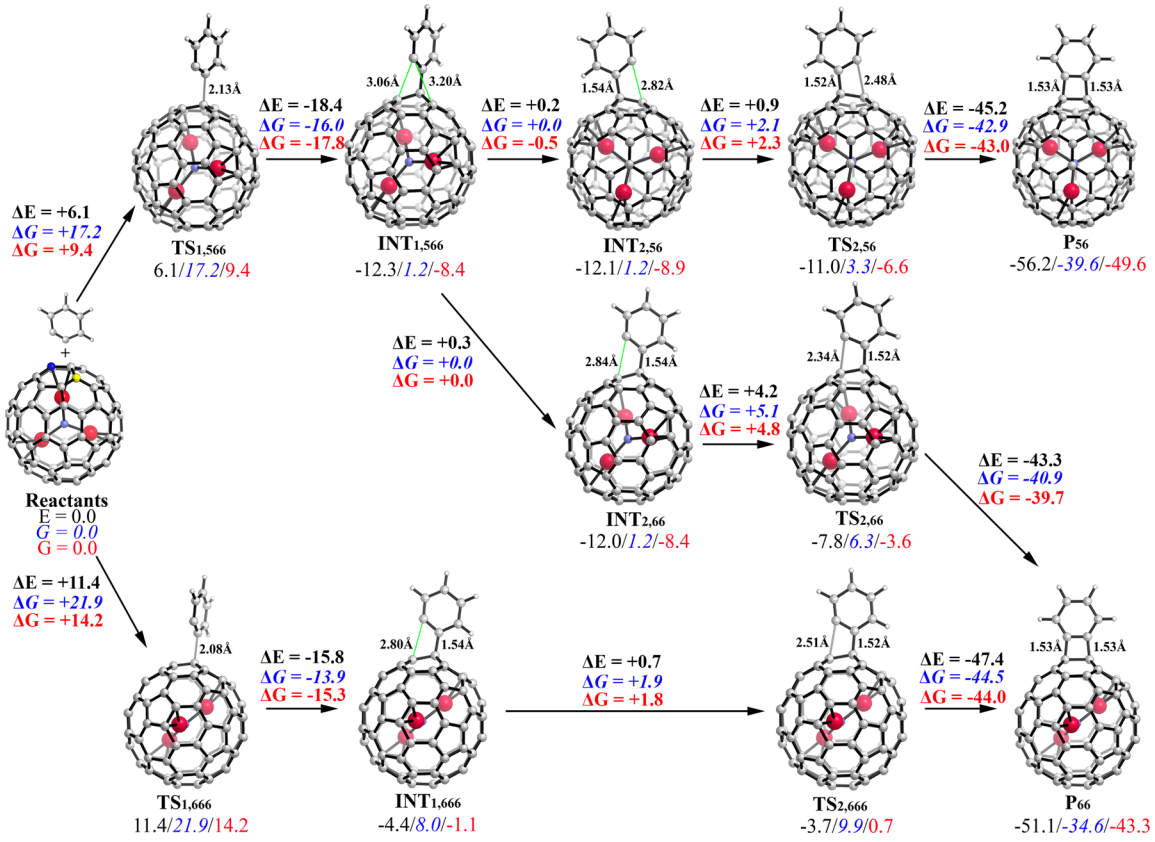

Figure 2. Energy profiles (in kcal/mol) of (2 + 2) cycloaddition of benzyne with $Sc_3N@C_{80}$. The different colors of energies are used to denote different levels of theory: electronic energies E at the B3LYP/Lanl2dz~6-311G(d,p) level, in black; Gibbs free energies G at the B3LYP/Lanl2dz~6-311G(d,p) level, in blue; Gibbs free energies G at the B3LYP-D3/Lanl2dz~6-311G(d,p) level, in red. The 566 and 666 sites are colored by blue and yellow in the reactants, respectively.

relatively low, indicating that the attack to 566 site is more preferred. After the transition states, singlet diradical intermediates $\mathbf{INT}_{1,566}$ and $\mathbf{INT}_{1,666}$ are formed.

For $\mathbf{INT}_{1,566}$, the unsaturated carbon atom in benzyne is above the hexagon, rather than the [5,6] or [6,6] bond of the fullerene surface. Interestingly, through rotating the carbon bond between the benzyne moiety and fullerenes, $\mathbf{INT}_{1,566}$ could isomerize to two new diradical intermediates $\mathbf{INT}_{2,56}$ and $\mathbf{INT}_{2,66}$. These three intermediates are essentially isoenergetic. Even though none transition state could be located between $\mathbf{INT}_1$ and $\mathbf{INT}_2$, the potential energy surface along the dihedral angle between benzyne moiety and [5,6] as well as [6,6] bonds were scanned theoretically. The calculation results showed that the energy change is less than 1 kcal/mol, and thus, the rotation of benzyne moiety on fullerene surface is almost barrierless (please see SI for more details). More importantly, the phenyl radical center is exactly over the [5,6] or [6,6] bond in $\mathbf{INT}_{2,56}$ and $\mathbf{INT}_{2,66}$. To form the final [5,6] ($\mathbf{P}_{56}$) and [6,6] ($\mathbf{P}_{66}$) products,[30] it is necessary for $\mathbf{INT}_{2,56}$ and $\mathbf{INT}_{2,66}$ to go through the transition states $\mathbf{TS}_{2,56}$ and $\mathbf{TS}_{2,66}$ respectively, both energy barriers of which are not high. On the other hand, the phenyl radical center in $\mathbf{INT}_{1,666}$ is rightly over the [6,6] bond. Thus, without any rotation, $\mathbf{INT}_{1,666}$ can go through $\mathbf{TS}_{2,666}$ directly and produce $\mathbf{P}_{66}$.

Consequently, the (2 + 2) cycloaddition of benzyne to $Sc_3N@C_{80}$ follows the diradical mechanism involving a conformationally flexible singlet diradical intermediate, rather than the carbene mechanism. The previously proposed singlet diradical pathway usually contains only one intermediate and two transition states. However, since the reaction mechanism at the 566 site involves two intermediates and two transition states, it cannot be simply regarded as the pathway **c**. The formation of the singlet diradical intermediate $\mathbf{INT}_{1,566}$, rather than the ring-closing step, is the rate-determining step for benzyne addition to $Sc_3N@C_{80}$. Furthermore, due to the lower energy height of $\mathbf{TS}_{2,56}$ with respect to $\mathbf{TS}_{2,66}$, the yield of $\mathbf{P}_{56}$ should be more than that of $\mathbf{P}_{66}$. Considering its barrier height and the reaction energy, $\mathbf{P}_{66}$ can also form, which accounts very well for the experimental observation that the yields of $\mathbf{P}_{56}$ and $\mathbf{P}_{66}$ are 70% and 15%, respectively.[5c]

Why does the (2 + 2) cycloaddition of benzyne to $Sc_3N@C_{80}$ involve such a novel rotatable diradical intermediate? This can be attributed to the inflexibility of both benzyne and $Sc_3N@$

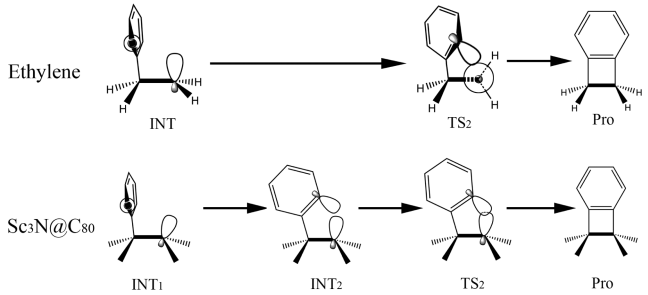

Figure 3. Schematic description of the orbital interaction of benzyne moiety with ethylene and $Sc_3N@C_{80}$ in the intermediates and second transition states. Other atoms in $Sc_3N@C_{80}$ are omitted for clarity.

DOI: 10.1021/jacs.5b01444
J. Am. Chem. Soc. 2015, 137, 6820−6828

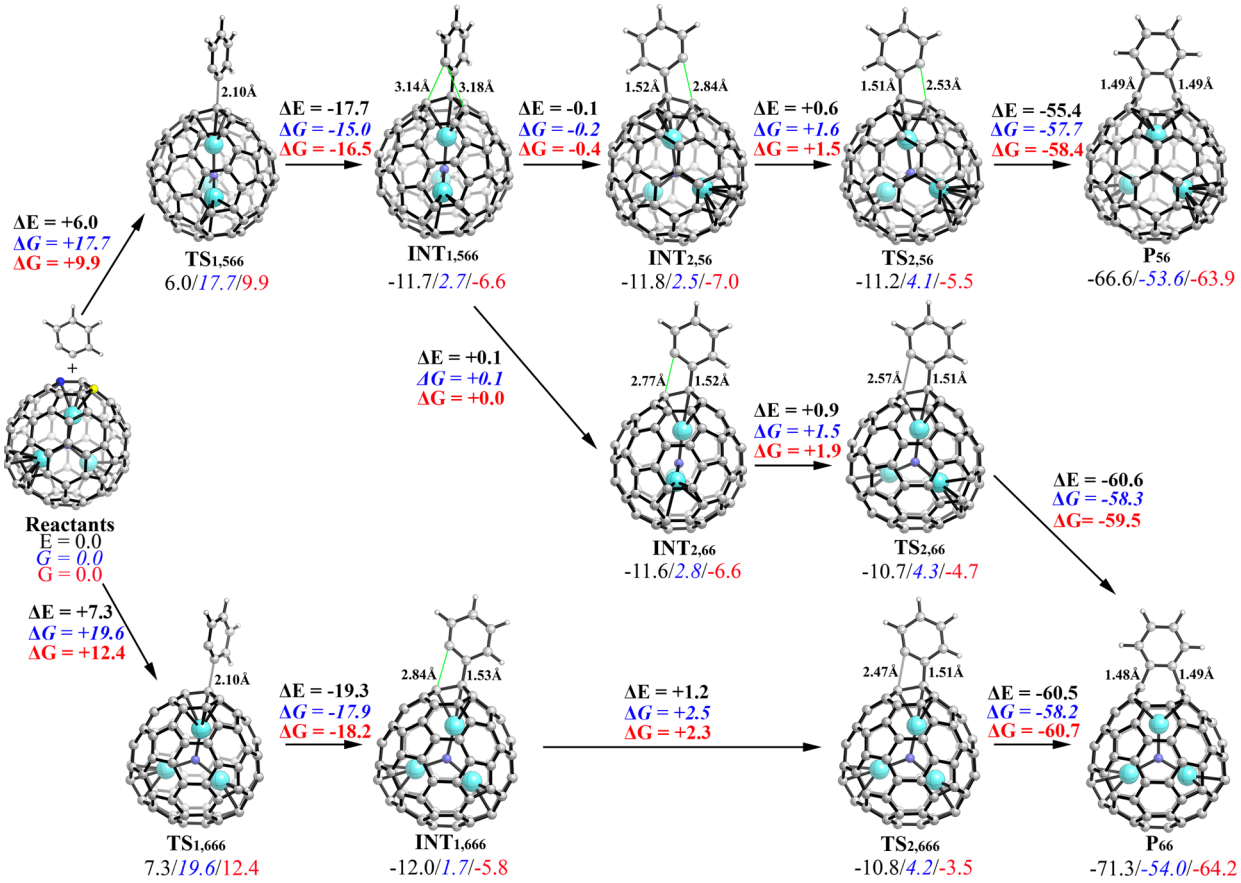

Figure 4. Energy profiles (in kcal/mol) of (2 + 2) cycloaddition of benzyne with $Y_3N@C_{80}$. The different colors of energies are used to denote different levels of theory: electronic energies E at the B3LYP/Lanl2dz~6-311G(d,p) level, in black; Gibbs free energies G at the B3LYP/Lanl2dz~6-311G(d,p) level, in blue; Gibbs free energies G at the B3LYP-D3/Lanl2dz~6-311G(d,p) level, in red. The 566 and 666 sites are colored by blue and yellow in the reactant, respectively.

C_{80}. To make this clearer, the cycloaddition of benzyne with ethylene is taken as a comparison. Figure 3 exhibits the orbital interaction of the diradical intermediate of benzyne addition to ethylene and $Sc_3N@C_{80}$. For ethylene, the orbital overlap can take place just by rotating the carbon bond of ethylene and bond between benzyne and ethylene; the transition state can be reached easily without formation of any other intermediate. However, due to the inflexibility of the fullerene, the carbon bond of the fullerene, along with the orbital, are fixed. To form the product, the benzyne moiety must rotate on the fullerene surface.

2. Reaction Mechanism of the (2 + 2) Cycloaddition of Benzyne to $Y_3N@C_{80}$. As shown in Figure 4, the reaction mechanism of cycloadditions of benzyne to $Y_3N@C_{80}$ also follows the diradical mechanism involving diradical intermediates. More interestingly, the $\mathbf{INT}_{1,566}$ could also isomerize to $\mathbf{INT}_{2,56}$ and $\mathbf{INT}_{2,66}$ through rotation of mono-σ bond between the benzyne moiety and fullerene.

Compared with $Sc_3N@C_{80}$, the energy barrier of $\mathbf{TS}_{1,566}$ of $Y_3N@C_{80}$ changes slightly but energy barrier of $\mathbf{TS}_{1,666}$ drops strongly. Moreover, the reaction energies increase obviously. Thus, $Y_3N@C_{80}$ has the higher chemical reactivity than $Sc_3N@C_{80}$. The thermodynamic stability between $\mathbf{P}_{56}$ and $\mathbf{P}_{66}$ is reversed, and $\mathbf{P}_{66}$ becomes more preferred thermodynamically.[30] Kinetically, $\mathbf{P}_{66}$ could also compete with $\mathbf{P}_{56}$, as a consequence of the similar energy barriers of the $\mathbf{TS}_{1,566}$ and $\mathbf{TS}_{1,666}$ as well as $\mathbf{TS}_{2,56}$ and $\mathbf{TS}_{2,66}$. It is reasonable to infer that both [5,6] and [6,6] $Y_3N@C_{80}$ benzoadducts are favorable. In the previous theoretical studies on Diels−Alder and 1,3-dipolar cycloadditions of $M_3N@C_{80}$, it is also found that for $Sc_3N@C_{80}$ the [5,6] bond is preferred over [6,6] bond whereas in the case of $Y_3N@C_{80}$, the [5,6] and [6,6] bonds have similar reactivity.[6b,e] Therefore, the endohedral cluster strongly influences the exohedral reactivity and regioselectivity of chemical reactions of $M_3N@C_{80}$, including (2 + 2), Diels−Alder, and 1,3-dipolar cycloadditions.

Unexpectedly, in both [5,6] and [6,6] $Y_3N@C_{80}$ benzoadducts, the C−C bond of the fullerene cage which involves in the cycloaddition reaction is broken, giving rise to the open-caged metallofullerenes with nine- and ten-numbered orifices. The distances of two carbon atoms are 2.397 and 2.488 Å respectively in both [5,6] and [6,6] benzoadducts, whereas the bond lengths of the corresponding C−C bond in the $Sc_3N@C_{80}$ benzoadducts are 1.659 and 1.668 Å. Interestingly, compared with the structures of $Sc_3N@C_{80}$ benzoadducts where the three scandium atoms are far away from the benzyne moiety, one of the encapsulated yttrium atom in $Y_3N@C_{80}$ benzoadducts points to the orifice. Especially, in [6,6] $Y_3N@C_{80}$ benzoadducts the metallic cluster Y_3N and the exohedral benzyne moiety are in the same plane.

Open-cage metallofullerenes, which usually stem from exohedral cycloadditions on EMFs, have been found recently.[1,2] Most open-cage metallofullerenes result from the opening of three-membered rings. Regarding the atom bridging the broken carbon bond in the fullerene skeleton, existing examples can be divided into fulleroids (methano-bridged annulene-type metal-

DOI: 10.1021/jacs.5b01444
J. Am. Chem. Soc. 2015, 137, 6820−6828

lofulleroids),[31] azafulleroids (aza-bridged annulene-type metallofulleroids),[3i] and silafulleroids (silylene-bridged annulene-type metallofulleroids).[32] Recently, Wang and co-workers reported that by introducing an additional oxygen atom, the carbon bond of four-numbered ring in the [5,6] $Sc_3N@C_{80}$ cycloadduct is ruptured, which is the first example of two atoms bridging open-cage metallofullerenes.[5d]

Our results show that the two-atom-bridging open-cage metallofullerenes can be easily realized without the aid of any other atom if $Y_3N@C_{80}$ is used as the reactant. Whether the cycloadduct is closed cage or open cage only depends on the endohedral metallic cluster. The (2 + 2) cycloaddition of benzyne on $M_3N@C_{80}$ (M = Sc, Y) is the first example where the endohedral cluster can control metallofullerene cycloadducts to be closed or open. This may stem from the fact that compared with other cycloadducts, the four-numbered ring from benzyne addition has modest strain energy and is very sensitive to the local strain energy of EMFs. The higher strain energy of EMFs, the larger likelihood of open-cage benzoadducts.

3. Origin of the Regioselectivity. Because of the rotating intermediate, $\mathbf{INT}_{1,566}$ could result in both $\mathbf{P}_{56}$ and $\mathbf{P}_{66}$ products. Therefore, the regioselectivity of $\mathbf{P}_{56}$ and $\mathbf{P}_{66}$ products depends on both the first C−C bond formation step and the ring-closing step, which correspond to the $\mathbf{TS}_1$ and $\mathbf{TS}_2$ respectively.

Due to the low LUMO energy level, benzyne is electrophilic and is attacked by the most nucleophilic carbons of the fullerene, which often have the highest negative charge. In EMFs, the charge transfer from the encapsulated atom(s) or cluster occurs mainly at the pentagons rather than on the hexagons,[33] causing the higher negative charge of the 566 site than the 666 site in $M_3N@C_{80}$. As shown in Table 1, the higher

Table 1. NBO Charge and POAV Values of the 566 and 666 Sites of Initial Reactants and $\mathbf{TS}_1$ of $M_3N@C_{80}$ (M = Sc, Y)

		NBO (reactant)	POAV (reactant)	POAV ($\mathbf{TS}_1$)
EMFs	site	lel	degree	degree
$Sc_3N@C_{80}$	566	−0.08	12.83	15.59
	666	−0.05	9.99	15.18
$Y_3N@C_{80}$	566	−0.11	14.37	17.53
	666	−0.04	11.68	16.90

NBO charge of the 566 site is conformity with the fact that $\mathbf{TS}_{1,566}$ shows lower energy barrier with respect to $\mathbf{TS}_{1,666}$. Nevertheless, NBO charge could not explain why $Y_3N@C_{80}$ has higher chemical reactivity than $Sc_3N@C_{80}$, especially for the energy barrier change of $\mathbf{TS}_{1,666}$.

As pointed out in previous works, the carbon atom with the large π-orbital axis vector (POAV)[34] values are highly reactive in the chemical reactions of fullerenes and EMFs, since the larger POAV value indicates that it is easier to deform the system from reactants to TS.[35] Table 1 also illustrates the POAV values of 566 and 666 sites of the initial reactants and $\mathbf{TS}_1$ of $M_3N@C_{80}$ (M = Sc, Y). The local strain curvature induced by pentagon and metallic cluster also gives rise to the larger POAV value of 566 site than that of 666 site, in agreement with the higher reactivity of 566 site. Furthermore, it is also evident that the large size of Y_3N cluster leads to the increment of POAV values, which accounts for the higher chemical reactivity of $Y_3N@C_{80}$. The increase of POAV value from reactant to $\mathbf{TS}_1$ reflects the further enlargement of the fullerene cage.

To further disclose the selectivity between $\mathbf{TS}_{1,566}$ and $\mathbf{TS}_{1,666}$, Houk's distortion/interaction model, which is also referred to as Bickelhaupt's activation strain model, is applied here.[36−38] The distortion/interaction model analyzes the relationship between energy barrier height and properties of reactants, and has been widely used to understand reaction rates and selectivities. In this model, the activation energy $\Delta E_a^{\ddagger}$ of the transition state can be decomposed as two parts: the distortion energy $\Delta E_{dis}^{\ddagger}$ and interaction energies $\Delta E_{int}^{\ddagger}$, as depicted in Figure 5. The distortion energies are the energies

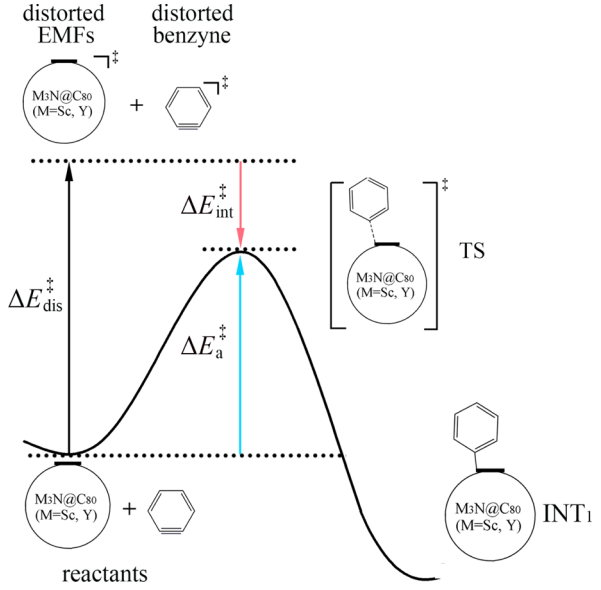

Figure 5. Relationship of activation energies $\Delta E_a^{\ddagger}$, distortion energies $\Delta E_{dis}^{\ddagger}$ and interaction energies $\Delta E_{int}^{\ddagger}$ in the distortion/interaction model.

needed to distort reactants from isolated geometries to the transition state geometries, while the interaction energy $\Delta E_{int}^{\ddagger}$ is the interaction energy between the distorted reactants. The relationship is defined as $\Delta E_a^{\ddagger} = \Delta E_{dis}^{\ddagger} + \Delta E_{int}^{\ddagger}$.

The calculated activation energies, distortion energies and interaction energies of $\mathbf{TS}_{1,566}$ and $\mathbf{TS}_{1,666}$ of $M_3N@C_{80}$ (M = Sc, Y) at the B3LYP/Lanl2dz~6-311G(d,p) level are presented in Figure 6. It is clear that all the four interaction energies ($\Delta E_{int}^{\ddagger}$) of these transition states are positive values, so the transition states are destabilized by interaction energies. For a given site, the $\Delta E_{int}^{\ddagger}$ are similar, 0.8−1.1 kcal/mol for $\mathbf{TS}_{1,566}$ and 2.4−2.6 kcal/mol for $\mathbf{TS}_{1,666}$, revealing that endohedral cluster has slightly effect on the interaction energy. On the other hand, the distortion energies $\Delta E_{dis}^{\ddagger}$ (5.3−8.8 kcal/mol) of $Sc_3N@C_{80}$ are much higher than those (4.9 kcal/mol) of $Y_3N@C_{80}$. It is reasonable to conclude that the distortion energy rather than interaction energy determines the chemical reactivity of $M_3N@C_{80}$ (M = Sc, Y) toward benzyne.

For $Sc_3N@C_{80}$, the $\Delta E_{dis}^{\ddagger}$ of $\mathbf{TS}_{1,666}$ is 8.8 kcal/mol, much higher than that of $\mathbf{TS}_{1,566}$ (5.3 kcal/mol). It is the large distortion energy as well as interaction energy of $\mathbf{TS}_{1,666}$ that bring about its higher energy barrier with respect to $\mathbf{TS}_{1,566}$. In the case of $Y_3N@C_{80}$, the $\Delta E_{dis}^{\ddagger}$ of $\mathbf{TS}_{1,566}$ and $\mathbf{TS}_{1,666}$ are same as 4.9 kcal/mol, thus, their energy barrier difference is

DOI: 10.1021/jacs.5b01444
J. Am. Chem. Soc. 2015, 137, 6820−6828

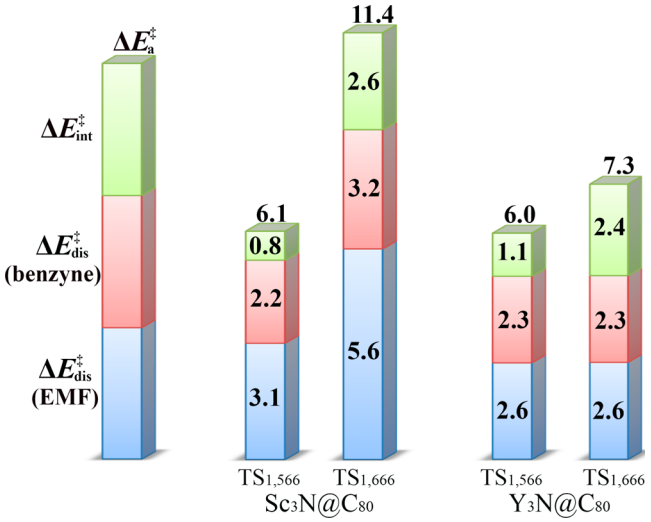

Figure 6. Activation energies $\Delta E_a^{\ddagger}$ (total height), distortion energies $\Delta E_{dis}^{\ddagger}$ of EMF (blue) and benzyne (red) and interaction energies $\Delta E_{int}^{\ddagger}$ (green) of $\mathbf{TS}_{1,566}$ and $\mathbf{TS}_{1,666}$ of $M_3N@C_{80}$ (M = Sc, Y) at the B3LYP/Lanl2dz~6-311G(d,p) level. The energy is in kcal/mol. The interaction energies are positive values, since interaction energies destabilize transition states.

determined by the interaction energy rather than distortion energy.

To answer why the energy barrier of $\mathbf{TS}_{1,666}$ changes so much from $Sc_3N@C_{80}$ to $Y_3N@C_{80}$, the geometry distortion of EMF from reactant to transition state is focused, because the distortion energy change mainly comes from $\Delta E_{dis}^{\ddagger}$ of EMF. As mentioned above, from reactant to $\mathbf{TS}_1$, the POAV value of reactive sites increases, indicating the enlargement of the fullerene cage. Interestingly, this has two opposite effects on the total distortion energy of EMFs: the increment of the strain energy of the fullerene cage, and the release of the strain energy of the endohedral metal cluster. Here, the POAV value of N atom in the metal cluster is used to reflect the strain energy of the metal cluster, as shown in Table 2.

Table 2. POAV Values of N Atom in the Metal Cluster M_3N (M = Sc, Y) of EMFs in Initial Reactant and TS_1 Geometries

	POAV (degree)		
EMFs	reactant	$\mathbf{TS}_{1,566}$	$\mathbf{TS}_{1,666}$
$Sc_3N@C_{80}$	0.78	0.61	0.78
$Y_3N@C_{80}$	6.01	3.64	1.64

Due to the small size of Sc_3N, the POAV value is close to zero and changes slightly in the $\mathbf{TS}_1$ geometries, suggesting that the strain energy of Sc_3N is very small. Therefore, from reactant to $\mathbf{TS}_1$, the strain energy of the fullerene cage increases, giving rise to the high distortion energy of EMF. On the other hand, the POAV value of 6.01° reveals that Y_3N is evidently compressed in C_{80}.[39] Nevertheless, the POAV reduces in the $\mathbf{TS}_1$ geometries, demonstrating that the strain energy of Y_3N is released. When $Y_3N@C_{80}$ transfers to $\mathbf{TS}_1$ geometries, the strain energy of the fullerene cage rises whereas the strain energy of Y_3N drops, leading to the lower total distortion energy of $Y_3N@C_{80}$ with respect to $Sc_3N@C_{80}$. Specially, the POAV value is only 1.64° in $\mathbf{TS}_{1,666}$ for $Y_3N@C_{80}$, which accounts for the fact that the distortion energy obviously reduces from 5.6 to 2.6 kcal/mol.

To explain the selectivity between $\mathbf{TS}_{2,56}$ and $\mathbf{TS}_{2,66}$ which correspond to the ring-closing step, the POAV values in three rotatable intermediates are depicted in Figure 7, as they belong

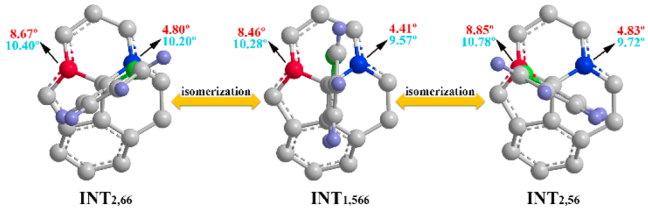

Figure 7. POAV values of 566 (red) and 666 (blue) sites in three rotatable intermediates of $M_3N@C_{80}$ (M = Sc, Y). The red and blue numbers are for $Sc_3N@C_{80}$ and $Y_3N@C_{80}$, respectively. The phenyl radical center is colored by green. Other atoms are omitted for clarity.

to the intramolecular transition state and are not suitable for the distortion/interaction model. For $Sc_3N@C_{80}$, no matter whether the intermediate is $\mathbf{INT}_{1,566}$, $\mathbf{INT}_{2,56}$ or $\mathbf{INT}_{2,56}$, the 566 site always shows much larger POAV value (angular distortion from planarity) with respect to the corresponding value of 666 site, in agreement with the higher reactivity of 566 site over 666 site. However, in the case of $Y_3N@C_{80}$, since the POAV values of 566 and 666 sites are similar in all three intermediates, the energy barrier heights of $\mathbf{TS}_{2,56}$ and $\mathbf{TS}_{2,66}$ are almost same. More importantly, as a consequence of the large size of the Y_3N cluster, the POAV values of $Y_3N@C_{80}$ increase significantly compared with those of $Sc_3N@C_{80}$, which can account for the much lower energy barriers of $\mathbf{TS}_{2,56}$ and $\mathbf{TS}_{2,66}$ of $Y_3N@C_{80}$.

4. (4 + 2) Cycloadducts of Benzyne with $M_3N@C_{80}$ (M = Sc, Y). From a theoretical point of view, benzyne addition to nanocarbon materials such as fullerenes, carbon nanotubes (CNTs) or graphene could generate two distinct products: (4 + 2) and (2 + 2) cycloadducts. For graphene, previous investigations indicated that (2 + 2) products are more favorable.[40] Benzyne addition to carbon nanotubes is quite interesting, and the chirality of the CNT plays a critical role; that is, for armchair single-walled carbon nanotubes (2 + 2) products are thermodynamically more stable than (4 + 2) ones, whereas benzyne prefers to form (4 + 2) cycloadducts on zigzag carbon nanotubes.[19e,41] For cycloaddition to fullerenes or EMFs, only the (2 + 2) product has been observed experimentally up to now. To further exclude the possibility of (4 + 2) products, we have theoretically investigated (4 + 2) cycloadducts of benzyne to $M_3N@C_{80}$ (M = Sc, Y).

As displayed in Figure 8, there are three possible (4 + 2) cycloadducts of benzyne addition to $M_3N@C_{80}$ (M = Sc, Y). According to the location of benzyne moiety, they can be classified into two categories; in $\mathbf{P}_{42,1}$, the benzyne moiety is attached to the pentagon whereas for $\mathbf{P}_{42,2}$ and $\mathbf{P}_{42,3}$ the moiety is attached to the hexagon. First, no matter which metallic cluster is encapsulated, the relative electronic energies ΔE and Gibbs free energies ΔG of (4 + 2) cycloadducts are much lower with respect to the corresponding (2 + 2) cycloadducts, revealing (4 + 2) cycloadducts are thermodynamically less stable, which agrees with the experimental fact that no (4 + 2) cycloadduct of benzyne with $Sc_3N@C_{80}$ was observed. Second, in contrast to the endothermicity of benzyne addition to the hexagon, benzyne addition to the pentagon is exothermic, which overcomes the large strain energy from the pentagon. Third, for $\mathbf{P}_{42,1}$ and $\mathbf{P}_{42,2}$ one and two carbon atoms connected

DOI: 10.1021/jacs.5b01444
J. Am. Chem. Soc. 2015, 137, 6820−6828

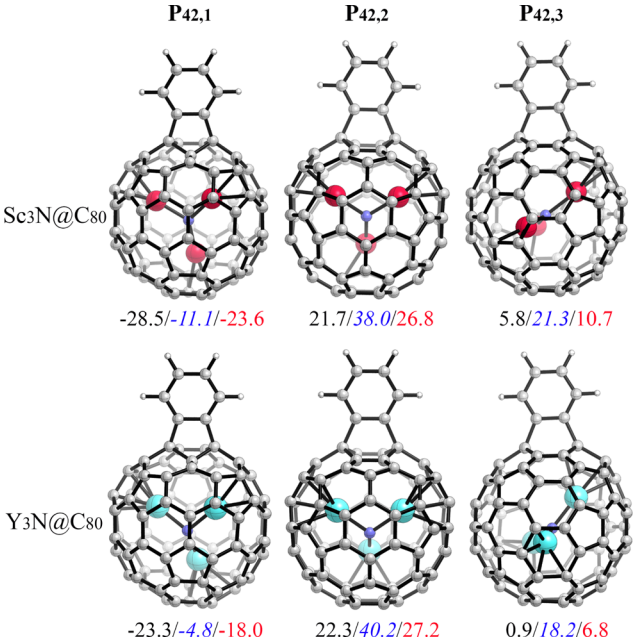

Figure 8. Three possible (4 + 2) cycloadducts of benzyne addition to $M_3N@C_{80}$ (M = Sc, Y). The different colors of energies with respect to isolated reactants are used to denote different levels of theory: electronic energies E at the B3LYP/Lanl2dz~6-311G(d,p) level, in black; Gibbs free energies G at the B3LYP/Lanl2dz~6-311G(d,p) level, in blue; Gibbs free energies G at the B3LYP-D3/Lanl2dz~6-311G(d,p) level, in red. The energy change is in kcal/mol.

to the reaction site bend out from the fullerene surface, in order to maintain the tetrahedral configuration of sp^3 carbon atoms. The large deformation of fullerene cages is responsible for the instability of (4 + 2) cycloadducts.

CONCLUSIONS

By means of theoretical calculations, we predict that (2 + 2) cycloadditions of benzyne to $M_3N@C_{80}$ (M = Sc, Y) follow the diradical mechanism and involve the formation of a singlet diradical intermediate. The reaction mechanism is influenced by the attack site of the first C−C bond formation step. Through rotation of the phenyl radical moiety on the fullerene surface, the singlet diradical intermediate on 566 site isomerizes to two new diradical intermediates, bringing about two distinct [5,6] and [6,6] benzoadducts. Thus, the reaction mechanism on 566 site involves two diradical intermediates and two transition states. On the other hand, the diradical intermediate on 666 site can only produce a [6,6] benzoadduct. The first C−C bond formation step is the rate-determining step while the selectivity between [5,6] and [6,6] benzoadducts depends on both the first C−C bond formation step and the ring-closing step. With the use of POAV values and the distortion/interaction model, the origin of regioselectivity is found to be the local strain energy of EMFs.

The nature of the endohedral cluster shows remarkable influence on the exohedral reactivity, regioselectivity, and cycloadduct geometry. From both kinetic and thermodynamic points of view, the [5,6] benzoadduct is slightly preferred for $Sc_3N@C_{80}$, which is in agreement with the experimental observation. In the case of $Y_3N@C_{80}$, [5,6] and [6,6] benzoadducts are competitive. More importantly, in contrast to closed-caged benzoadducts of $Sc_3N@C_{80}$, the four-membered ring of $Y_3N@C_{80}$ benzoadducts are open rather than closed. Therefore, (2 + 2) cycloaddition of benzyne to $M_3N@C_{80}$ (M = Sc, Y) is the first example that the preference for closed cage or open cage adducts is controlled by the endohedral metallic cluster. Further calculations on (4 + 2) cycloadducts of benzyne with $M_3N@C_{80}$ (M = Sc, Y) confirmed that they are thermodynamically less stable than (2 + 2) cycloadducts.

Since the $Y_3N@C_{80}$ exhibits higher chemical reactivity in (2 + 2) cycloaddition compared with $Sc_3N@C_{80}$, the open-caged $Y_3N@C_{80}$ benzoadducts could be synthesized experimentally in future. Our work will not only encourage further experimental and theoretical research on chemical functionalization of fullerene, but also enrich the understanding of (2 + 2) cycloaddition in organic chemistry.

ASSOCIATED CONTENT

Supporting Information

Test calculations on (2 + 2) cycloaddition of benzyne and ethylene; relative energies of three-numbered ring structures of benzyne with EMFs; B3LYPD and mPW1PW91 results; full reference of ref 27; relative electronic energies of regioisomers; the rotation energy change along the dihedral angle between benzyne moiety and [5,6] as well as [6,6] bonds in intermediates of $Sc_3N@C_{80}$; energies and Cartesian coordinates of the reactants, transition states, intermediates, and products of cycloaddition reactions of benzyne on $M_3N@C_{80}$ (M = Sc, Y). The Supporting Information is available free of charge on the ACS Publications website at DOI: 10.1021/jacs.5b01444.

AUTHOR INFORMATION

Corresponding Authors

*xzhao@mail.xjtu.edu.cn.
*houk@chem.ucla.edu.

Notes

The authors declare no competing financial interests.

ACKNOWLEDGMENTS

This work was financially supported by the National Natural Science Foundation of China (21171138, 20673081), the National Key Basic Research Program of China (2012CB720904), and the National Science Foundation of the U.S.A. (CHE-1361104).

REFERENCES

(1) (a) *Endofullerenes: A New Family of Carbon Clusters*; Akasaka, T., Nagase, S., Eds.; Kluwer Academic Publishers: Dordrecht, 2002. (b) Martín, N. *Chem. Commun.* **2006**, 2093. (c) Dunsch, L.; Yang, S. *Small* **2007**, *3*, 1298. (d) Chaur, M. N.; Melin, F.; Ortiz, A. L.; Echegoyen, L. *Angew. Chem., Int. Ed.* **2009**, *48*, 7514. (e) Tan, Y.-Z.; Xie, S.-Y.; Huang, R.-B.; Zheng, L.-S. *Nat. Chem.* **2009**, *1*, 450. (f) Rodríguez-Fortea, A.; Balch, A. L.; Poblet, J. M. *Chem. Soc. Rev.* **2011**, *40*, 3551. (g) *Chemistry of Nanocarbons*; Akasaka, T., Wudl, F., Nagase, S., Eds.; John Wiley & Sons: Chichester, U.K., 2010. (h) Yang, S.; Liu, F.; Chen, C.; Jiao, M.; Wei, T. *Chem. Commun.* **2011**, *47*, 11822. (i) Lu, X.; Feng, L.; Akasaka, T.; Nagase, S. *Chem. Soc. Rev.* **2012**, *41*, 7723. (j) Zhang, J.; Stevenson, S.; Dorn, H. C. *Acc. Chem. Res.* **2013**, *46*, 1548. (k) Popov, A. A.; Yang, S.; Dunsch, L. *Chem. Rev.* **2013**, *113*, 5989. (l) Wang, T.; Wang, C. *Acc. Chem. Res.* **2014**, *47*, 450.

(2) (a) Yamada, M.; Akasaka, T.; Nagase, S. *Acc. Chem. Res.* **2010**, *43*, 92. (b) Osuna, S.; Swart, M.; Solá, M. *Phys. Chem. Chem. Phys.* **2011**, *13*, 3585. (c) Lu, X.; Akasaka, T.; Nagase, S. *Chem. Commun.* **2011**, *47*, 5942. (d) Yamada, M.; Akasaka, T.; Nagase, S. *Chem. Rev.* **2013**, *113*, 7209. (e) Garcia-Borràs, M.; Osuna, S.; Luis, J. M.; Swart, M.; Solà, M.

DOI: 10.1021/jacs.5b01444
J. Am. Chem. Soc. 2015, 137, 6820−6828

Chem. Soc. Rev. **2014**, *43*, 5089. (f) Lu, X.; Bao, L.; Akasaka, T.; Nagase, S. *Chem. Commun.* **2014**, *50*, 14701.
(3) Some examples of chemical reactions of EMFs (a) Akasaka, T.; Kato, T.; Kobayashi, K.; Nagase, S.; Yamamoto, K.; Funasaka, H.; Takahashi, T. *Nature* **1995**, *374*, 600. (b) Suzuki, T.; Maruyama, Y.; Kato, T.; Akasaka, T.; Kobayashi, K.; Nagase, S.; Yamamoto, K.; Funasaka, H.; Takahashi, T. *J. Am. Chem. Soc.* **1995**, *117*, 9606. (c) Iezzi, E. B.; Duchamp, J. C.; Harich, K.; Glass, T. E.; Lee, H. M.; Olmstead, M. M.; Balch, A. L.; Dorn, H. C. *J. Am. Chem. Soc.* **2002**, *124*, 524. (d) Cao, B. P.; Wakahara, T.; Maeda, Y.; Han, A. H.; Akasaka, T.; Kato, T.; Kobayashi, K.; Nagase, S. *Chem.—Eur. J.* **2004**, *10*, 716. (e) Bolskar, R. D.; Benedetto, A. F.; Husebo, L. O.; Price, R. E.; Jackson, E. F.; Wallace, S.; Wilson, L. J.; Alford, J. M. *J. Am. Chem. Soc.* **2003**, *125*, 5471. (f) Cai, T.; Ge, Z. X.; Iezzi, E. B.; Glass, T. E.; Harich, K.; Gibson, H. W.; Dorn, H. C. *Chem. Commun.* **2005**, 3594. (g) Cardona, C. M.; Kitaygorodskiy, A.; Echegoyen, L. *J. Am. Chem. Soc.* **2005**, *127*, 10448. (h) Cardona, C. M.; Kitaygorodskiy, A.; Ortiz, A.; Herranz, M. A.; Echegoyen, L. *J. Org. Chem.* **2005**, *70*, 5092. (i) Liu, T.-X.; Wei, T.; Zhu, S.-E.; Wang, G.-W.; Jiao, M.; Yang, S.; Bowles, F. L.; Olmstead, M. M.; Balch, A. L. *J. Am. Chem. Soc.* **2012**, *134*, 11956. (j) Sawai, K.; Takano, Y.; Izquierdo, M.; Filippone, S.; Martín, N.; Slanina, Z.; Mizorogi, N.; Waelchli, M.; Tsuchiya, T.; Akasaka, T.; Nagase, S. *J. Am. Chem. Soc.* **2011**, *133*, 17746. (k) Maroto, E. E.; Izquierdo, M.; Murata, M.; Filippone, S.; Komatsu, K.; Murata, Y.; Martín, N. *Chem. Commun.* **2014**, *50*, 740. (l) Maroto, E. E.; Mateos, J.; Garcia-Borràs, M.; Osuna, S.; Filippone, S.; Herranz, M. A.; Murata, Y.; Solà, M.; Martín, N. *J. Am. Chem. Soc.* **2015**, *137*, 1190 Please see more examples from refs 1 and 2.
(4) (a) Hoke, S. H., II; Molstad, J.; Dilettato, D.; Jay, M. J.; Carlson, D.; Kahr, B.; Cooks, R. G. *J. Org. Chem.* **1992**, *57*, 5069. (b) Meier, M. S.; Wang, G.-W.; Haddon, R. C.; Brock, C. P.; Lloyd, M. A.; Selegue, J. P. *J. Am. Chem. Soc.* **1998**, *120*, 2337.
(5) (a) Lu, X.; Xu, J. X.; He, X. R.; Shi, Z. J.; Gu, Z. N. *Chem. Mater.* **2004**, *16*, 953. (b) Lu, X.; Nikawa, H.; Tsuchiya, T.; Akasaka, T.; Toki, M.; Sawa, H.; Mizorogi, N.; Nagase, S. *Angew. Chem., Int. Ed.* **2010**, *49*, 594. (c) Li, F.-F.; Pinzón, J. R.; Mercado, B. Q.; Olmstead, M. M.; Balch, A. L.; Echegoyen, L. *J. Am. Chem. Soc.* **2011**, *133*, 1563. (d) Wang, G.; Liu, T.; Jiao, M.; Wang, N.; Zhu, S.; Chen, C.; Yang, S.; Bowles, F. L.; Beavers, C. M.; Olmstead, M. M.; Mercado, B. Q.; Balch, A. L. *Angew. Chem., Int. Ed.* **2011**, *50*, 4658.
(6) (a) Campanera, J. M.; Bo, C.; Poblet, J. M. *J. Org. Chem.* **2006**, *71*, 46. (b) Cai, T.; Slebodnick, C.; Xu, L.; Harich, K.; Glass, T. E.; Chancellor, C.; Fettinger, J. C.; Olmstead, M. M.; Balch, A. L.; Gibson, H. W.; Dorn, H. C. *J. Am. Chem. Soc.* **2006**, *128*, 6486. (c) Rodriguez-Fortea, A.; Campanera, J. M.; Cardona, C. M.; Echegoyen, L.; Poblet, J. M. *Angew. Chem., Int. Ed.* **2006**, *45*, 8176. (d) Aroua, S.; Yamakoshi, Y. *J. Am. Chem. Soc.* **2012**, *134*, 20242. (e) Garcia-Borràs, M.; Osuna, S.; Luis, J. M.; Swart, M.; Solà, M. *Chem.—Eur. J.* **2013**, *19*, 14931.
(7) Popov, A. A.; Pykhova, A. D.; Ioffe, I. N.; Li, F.-F.; Echegoyen, L. *J. Am. Chem. Soc.* **2014**, *136*, 13436.
(8) Woodward, R. B.; Hoffmann, R. *Angew. Chem., Int. Ed. Engl.* **1969**, *8*, 781.
(9) (a) Laird, D. W.; Gilbert, J. C. *J. Am. Chem. Soc.* **2001**, *123*, 6704. (b) Bachrach, S. M.; Gilbert, J. C.; Laird, D. W. *J. Am. Chem. Soc.* **2001**, *123*, 6706. (c) Bachrach, S. M.; Gilbert, J. C. *J. Org. Chem.* **2004**, *69*, 6357.
(10) (a) Ozkan, I.; Kinal, A. *J. Org. Chem.* **2004**, *69*, 5390. (b) Kinal, A.; Piecuch, P. *J. Phys. Chem. A* **2006**, *110*, 367. (c) Bronner, S. M.; Mackey, J. L.; Houk, K. N.; Garg, N. K. *J. Am. Chem. Soc.* **2012**, *134*, 13966. (d) Medina, J. M.; Mackey, J. L.; Garg, N. K.; Houk, K. N. *J. Am. Chem. Soc.* **2014**, *136*, 15798.
(11) (a) Martín, N.; Altable, M.; Filippone, S.; Martín-Domenech, A.; Güell, M.; Solà, M. *Angew. Chem., Int. Ed.* **2006**, *45*, 1439. (b) Altable, M.; Filippone, S.; Martín-Domenech, A.; Güell, M.; Solà, M.; Martín, N. *Org. Lett.* **2006**, *8*, 5959. (c) Güell, M.; Martín, N.; Altable, M.; Filippone, S.; Martín-Domenech, A.; Solà, M. *J. Phys. Chem. A* **2007**, *111*, 5253.
(12) (a) Lu, X. *J. Am. Chem. Soc.* **2003**, *125*, 6384. (b) Yao, Z.-K.; Yu, Z.-X. *J. Am. Chem. Soc.* **2011**, *133*, 10864. (c) Siebert, M. R.; Osbourn, J. M.; Brummond, K. M.; Tantillo, D. J. *J. Am. Chem. Soc.* **2010**, *132*, 11952. (d) Sio, V.; Harrison, J. G.; Tantillo, D. J. *Tetrahedron Lett.* **2012**, *53*, 6919.
(13) Chen, N.; Zhang, E.-Y.; Tan, K.; Wang, C.; Lu, X. *Org. Lett.* **2007**, *9*, 2011.
(14) (a) Becke, A. D. *Phys. Rev. A* **1988**, *38*, 3098. (b) Lee, C.; Yang, W.; Parr, R. G. *Phys. Rev. B* **1988**, *37*, 785. (c) Becke, A. D. *J. Chem. Phys.* **1993**, *98*, 5648.
(15) Hay, P. J.; Wadt, W. R. *J. Chem. Phys.* **1985**, *82*, 299.
(16) (a) Osuna, S.; Swart, M.; Solà, M. *J. Phys. Chem. A* **2011**, *115*, 3491. (b) Fokin, A. A.; Chernish, L. V.; Gunchenko, P. A.; Tikhonchuk, E. Y.; Hausmann, H.; Serafin, M.; Dahl, J. E.; Carlson, R. M.; Schreiner, P. R. *J. Am. Chem. Soc.* **2012**, *134*, 13641. (c) Garcia-Borras, M.; Osuna, S.; Swart, M.; Luis, J. M.; Solà, M. *Chem. Commun.* **2013**, *49*, 1220. (d) Cao, Y.; Liang, Y.; Zhang, L.; Osuna, S.; Hoyt, A.-L. M.; Briseno, A. L.; Houk, K. N. *J. Am. Chem. Soc.* **2014**, *136*, 10743.
(17) (a) Bartlett, R. J.; Purvis, G. D., III. *Int. J. Quantum Chem.* **1978**, *14*, 561. (b) Pople, J. A.; Head-Gordon, M.; Raghavachari, K. *J. Chem. Phys.* **1987**, *87*, 5968.
(18) (a) Knowles, P. J.; Werner, H.-J. *Chem. Phys. Lett.* **1985**, *115*, 259. (b) Werner, H.-J.; Knowles, P. J. *J. Chem. Phys.* **1985**, *82*, 5053.
(19) (a) Bendikov, M.; Duong, H. M.; Starkey, K.; Houk, K. N.; Carter, E. A.; Wudl, F. *J. Am. Chem. Soc.* **2004**, *126*, 7416. (b) Zhao, Y.-L.; Suhrada, C. P.; Jung, M. E.; Houk, K. N. *J. Am. Chem. Soc.* **2006**, *128*, 11106. (c) Lovitt, C. F.; Dong, H.; Hrovat, D. A.; Gleiter, R.; Borden, W. T. *J. Am. Chem. Soc.* **2010**, *132*, 14617. (d) Gao, X.; Hodgson, J. L.; Jiang, D.; Zhang, S. B.; Nagase, S.; Miller, G. P.; Chen, Z. *Org. Lett.* **2011**, *13*, 3316. (e) Yang, T.; Zhao, X.; Nagase, S. *Org. Lett.* **2013**, *15*, 5960. (f) James, N. C.; Um, J. M.; Padias, A. B.; Hall, H. K., Jr.; Houk, K. N. *J. Org. Chem.* **2013**, *78*, 6582.
(20) (a) Grimme, S. *J. Comput. Chem.* **2004**, *25*, 1463. (b) Grimme, S. *J. Comput. Chem.* **2006**, *27*, 1787.
(21) (a) Haberhauer, G.; Gleiter, R. *J. Am. Chem. Soc.* **2013**, *135*, 8022. (b) Fabig, S.; Haberhauer, G.; Gleiter, R. *J. Am. Chem. Soc.* **2015**, *137*, 1833.
(22) In the calculations on (2 + 2) cycloaddition of benzyne and ethylene, we tested a series of popular density functionals. It is found that, among those density functonals, B3LYP gives the closest results to those from B2PLYPD. Please see SI for more details.
(23) The Grimme's dispersion correction in B3LYPD can be invoked by the keyword of IOP(3/124=3) in *Gaussian 09*, Revision B01.
(24) (a) Grimme, S.; Antony, J.; Ehrlich, S.; Krieg, H. *J. Chem. Phys.* **2010**, *132*, 154104. (b) Grimme, S.; Ehrlich, S.; Goerigk, L. *J. Comput. Chem.* **2011**, *32*, 1456.
(25) Adamo, C.; Barone, V. *J. Chem. Phys.* **1998**, *108*, 664.
(26) Glendening, E. D.; Reed, A. E.; Carpenter, J. E.; Weinhold, F. *NBO*, version 3.1; University of Wisconsin: Madison, WI, 1996.
(27) (a) Frisch, M. J.; et al. *Gaussian 09*, Revision A.01; Gaussian, Inc.: Wallingford, CT, 2009. (b) Frisch, M. J.; et al. *Gaussian 09*, Revision B.01; Gaussian, Inc.: Wallingford, CT, 2010. See SI for full references.
(28) Grimme, S. *DFTD3*, V3.1 Rev 0; University Münster: Münster, Germany, 2014.
(29) Legault, C. Y. *CYLView*, 1.0b; Universitéde Sherbrooke, Canada, 2009; http://www.cylview.org.
(30) For [5,6] and [6,6] benzoadducts, we systematically calculated about ten orientations of the cluster inside the fullerene cage with respect to the C-C bond involved in cycloaddition. For $Sc_3N@C_{80}$, it is clear that the cluster rotates more easily in the [6,6] benzoadducts than in the [5,6] one, as several isoenergetic orientations are found, which agrees with recent calculation results from Popov et al. (see ref 7.). For $Y_3N@C_{80}$, the endohedral cluster is fixed due to the large energy barriers of rotation inside the fullerene cage. For details, please see the SI.
(31) (a) Shu, C.; Cai, T.; Xu, L.; Zuo, T.; Reid, J.; Harich, K.; Dorn, H. C.; Gibson, H. W. *J. Am. Chem. Soc.* **2007**, *129*, 15710. (b) Shu, C.; Xu, W.; Slebodnick, C.; Champion, H.; Fu, W.; Reid, J. E.; Azurmendi, H.; Wang, C.; Harich, K.; Dorn, H. C.; Gibson, H. W. *Org. Lett.* **2009**, *11*, 1753. (c) Lukoyanova, O.; Cardona, C. M.; Rivera, J.; Lugo-

DOI: 10.1021/jacs.5b01444
J. Am. Chem. Soc. 2015, 137, 6820−6828

Morales, L. Z.; Chancellor, C. J.; Olmstead, M. M.; Rodíguez-Fortea, A.; Poblet, J. M.; Balch, A. L.; Echegoyen, L. *J. Am. Chem. Soc.* **2007**, *129*, 10423. (d) Maeda, Y.; Matsunaga, Y.; Wakahara, T.; Takahashi, S.; Tsuchiya, T.; Ishitsuka, M. O.; Hasegawa, T.; Akasaka, T.; Liu, M. T. H.; Kokura, K.; Horn, E.; Yoza, K.; Kato, T.; Okubo, S.; Kobayashi, K.; Nagase, S.; Yamamoto, K. *J. Am. Chem. Soc.* **2004**, *126*, 6858. (e) Lu, X.; Nikawa, H.; Nakahodo, T.; Tsuchiya, T.; Ishitsuka, M. O.; Maeda, Y.; Akasaka, T.; Toki, M.; Sawa, H.; Slanina, Z.; Mizorogi, N.; Nagase, S. *J. Am. Chem. Soc.* **2008**, *130*, 9129. (f) Lu, X.; Nikawa, H.; Tsuchiya, T.; Maeda, Y.; Ishitsuka, M. O.; Akasaka, T.; Toki, M.; Sawa, H.; Slanina, Z.; Mizorogi, N.; Nagase, S. *Angew. Chem., Int. Ed.* **2008**, *47*, 8642.

(32) Sato, K.; Kako, M.; Suzuki, M.; Mizorogi, N.; Tsuchiya, T.; Olmstead, M. M.; Balch, A. L.; Akasaka, T.; Nagase, S. *J. Am. Chem. Soc.* **2012**, *134*, 16033.

(33) (a) Rodríguez-Fortea, A.; Alegret, N.; Balch, A. L.; Poblet, J. M. *Nat. Chem.* **2010**, *2*, 955. (b) Garcia-Borràs, M.; Osuna, S.; Swart, M.; Luis, J. M.; Solà, M. *Angew. Chem., Int. Ed.* **2013**, *52*, 9275.

(34) Haddon, R. C.; Chow, S. Y. *J. Am. Chem. Soc.* **1998**, *120*, 10494.

(35) (a) Solà, M.; Mestres, J.; Duran, M. *J. Phys. Chem. A* **1995**, *99*, 10752. (b) Osuna, S.; Swart, M.; Campanera, J. M.; Poblet, J. M.; Solà, M. *J. Am. Chem. Soc.* **2008**, *130*, 6206. (c) Osuna, S.; Swart, S.; Solà, M. *J. Am. Chem. Soc.* **2009**, *131*, 129. (d) Dang, J.-S.; Zheng, J.-J.; Wang, W.-W.; Zhao, X. *Inorg. Chem.* **2013**, *52*, 4762. (e) Yang, T.; Zhao, X.; Nagase, S.; Akasaka, T. *Chem.- Asian J.* **2014**, *9*, 2604.

(36) (a) Ess, D. H.; Houk, K. N. *J. Am. Chem. Soc.* **2007**, *129*, 10646. (b) Ess, D. H.; Houk, K. N. *J. Am. Chem. Soc.* **2008**, *130*, 10187.

(37) For reviews of activation strain model, please see: (a) van Zeist, W.-J.; Bickelhaupt, F. M. *Org. Biomol. Chem.* **2010**, *8*, 3118. (b) Fernández, I.; Bickelhaupt, F. M. *Chem. Soc. Rev.* **2014**, *43*, 4953.

(38) For some recent examples of the distortion/interaction model, please see: (a) Fernandez, I.; Solà, M.; Bickelhaupt, F. M. *Chem.—Eur. J.* **2013**, *19*, 7416. (b) Usharani, D.; Lacy, D. C.; Borovik, A. S.; Shaik, S. *J. Am. Chem. Soc.* **2013**, *135*, 17090. (c) Lopez, S. A.; Houk, K. N. *J. Org. Chem.* **2013**, *78*, 1778. (d) Yang, T.; Zhao, X.; Nagase, S. *J. Comput. Chem.* **2013**, *34*, 2223. (e) Liu, F.; Liang, Y.; Houk, K. N. *J. Am. Chem. Soc.* **2014**, *136*, 11483. (f) Yang, Y.-F.; Cheng, G.-J.; Liu, P.; Leow, D.; Sun, T.-Y.; Chen, P.; Zhang, X.; Yu, J.-Q.; Wu, Y.-D.; Houk, K. N. *J. Am. Chem. Soc.* **2014**, *136*, 344. (g) Medina, J. M.; Mackey, J. L.; Garg, N. K.; Houk, K. N. *J. Am. Chem. Soc.* **2014**, *136*, 15798.

(39) The compression of the metal cluster in $M_3N@C_{80}$ (M = Sc, Y) was also discussed in: Deng, Q.; Popov, A. A. *J. Am. Chem. Soc.* **2014**, *136*, 4257.

(40) Denis, P. A.; Iribarne, F. *J. Mater. Chem.* **2012**, *22*, 5470.

(41) Criado, A.; Vizuete, M.; Gómez-Escalonilla, M. J.; García-Rodriguez, S.; Fierro, J. L. G.; Cobas, A.; Peña, D.; Guitián, E.; Langa, F. *Carbon* **2013**, *63*, 140.

■ NOTE ADDED AFTER ASAP PUBLICATION

This paper was published ASAP on May 22, 2015. The last sentence on the first page of the Article has been corrected. The revised version posted on June 3, 2015.

DOI: 10.1021/jacs.5b01444
J. Am. Chem. Soc. 2015, 137, 6820−6828